The Plant Cell, Vol. 17, 525–536, February 2005, www.plantcell.org © 2005 American Society of Plant Biologists

Dissection of Arabidopsis ADP-RIBOSYLATION FACTOR 1 Function in Epidermal Cell Polarity [W]

Jian Xu and Ben Scheres[1]

Department of Molecular Cell Biology, Utrecht University, 3584 CH Utrecht, The Netherlands

Vesicle trafficking is essential for the generation of asymmetries, which are central to multicellular development. Core components of the vesicle transport machinery, such as ADP-ribosylation factor (ARF) GTPases, have been studied primarily at the single-cell level. Here, we analyze developmental functions of the *ARF1* subclass of the *Arabidopsis thaliana* multigene *ARF* family. Six virtually identical *ARF1* genes are ubiquitously expressed, and single loss-of-function mutants in these genes reveal no obvious developmental phenotypes. Fluorescence colocalization studies reveal that ARF1 is localized to the Golgi apparatus and endocytic organelles in both onion (*Allium cepa*) and Arabidopsis cells. Apical-basal polarity of epidermal cells, reflected by the position of root hair outgrowth, is affected when ARF1 mutants are expressed at early stages of cell differentiation but after they exit mitosis. Genetic interactions during root hair tip growth and localization suggest that the ROP2 protein is a target of ARF1 action, but its localization is slowly affected upon ARF1 manipulation when compared with that of Golgi and endocytic markers. Localization of a second potential target of ARF1 action, PIN2, is also affected with slow kinetics. Although extreme redundancy precludes conventional genetic dissection of ARF1 functions, our approach separates different ARF1 downstream networks involved in local and specific aspects of cell polarity.

INTRODUCTION

The generation of polarity within cells is crucial for cell intrinsic functions, such as localized protein secretion and cell division. In addition, cell polarity plays multiple roles in the multicellular context, for example, in the partitioning of fate determinants during asymmetric cell division. Asymmetries for both cell-intrinsic and developmental purposes in yeast and animal systems depend on vesicle trafficking (Mostov et al., 2003). Genetic screens have revealed specific regulators of vesicle trafficking in animal and plants (see below), but core factors, such as ADP-ribosylation factors (ARFs), have mainly been studied in cultured cells.

ARF family members cycle between an active GTP-bound and an inactive GDP-bound state. A subset of ARF proteins is referred to as class 1 based on their sequence conservation, and these proteins regulate intracellular vesicular trafficking at multiple stages of the secretory and lysosomal/vacuolar transport pathways in mammalian and plant cells (Balch et al., 1992; Lee et al., 2002; Presley et al., 2002; Takeuchi et al., 2002; Pimpl et al., 2003). In particular, class 1 ARF proteins participate in the formation of transport vesicles and the selection of transmembrane protein cargo from donor compartments in mammalian cells (Goldberg, 2000; Spang, 2002).

The vesicle transport inhibitor brefeldin A (BFA) has been shown to interfere with ARF action in mammalian, fungal, and plant cells (Chardin and McCormick, 1999; Nebenfuhr et al., 2002). BFA inhibits the rate of guanine nucleotide exchange exhibited by ARF1 and interferes with ARF1 function in COPI coat recruitment. Crystal structure of the ARF1-GDP/Sec7/BFA complex shows that BFA binds at the protein–protein interface to inhibit conformational changes in ARF1 required for Sec7 to dislodge the GDP molecule (Mossessova et al., 2003). BFA induces redistribution of Golgi proteins into the endoplasmic reticulum (ER) in mammalian and plant cells (Lippincott-Schwartz et al., 1989; Saint-Jore et al., 2002). Moreover, interference of BFA with the endocytic pathways in animals and plants has been reported (Lippincott-Schwartz et al., 1991; Geldner et al., 2003; Grebe et al., 2003). BFA also interferes with cell polarity in plants, in which it disturbs zygote polarity in Fucus (Shaw and Quatrano, 1996), randomizes the root hair initiation site of *Arabidopsis thaliana* trichoblast cells, and interferes with the localization of putative auxin efflux carrier components of the PIN family and auxin influx carrier AUX1 (Geldner et al., 2001; Grebe et al., 2002).

Consistent with a potential role for the ARF proteins in the establishment of plant cell polarity, mutations in BFA-sensitive Arabidopsis GNOM/EMB30 ARF-GEF (guanine nucleotide exchange factor) lead to aberrant cell shape and orientation of cell division (Mayer et al., 1993; Shevell et al., 1994). GNOM/EMB30 protein localizes to endocytic organelles, and one of its functions is to control the polarized trafficking of the BFA-sensitive auxin efflux component PIN1 to the basal plasma membrane (Steinmann et al., 1999; Geldner et al., 2003).

[1] To whom correspondence should be addressed. E-mail b.scheres@bio.uu.nl; fax 31-30-251-3655.

The author responsible for distribution of materials integral to the findings presented in this article in accordance with the policy described in the Instructions for Authors (www.plantcell.org) is: Ben Scheres (b.scheres@bio.uu.nl).

[W] Online version contains Web-only data.

Article, publication date, and citation information can be found at www.plantcell.org/cgi/doi/10.1105/tpc.104.028449.

Additional targets for ARF-dependent vesicle trafficking are suggested by the observation that BFA inhibits early polar localization of ROP (RHO of plants) proteins at the root hair initiation site (Molendijk et al., 2001). ROP proteins are homologs of the RHO/RAC/CDC42, members of the RHO family GTPases, which include key regulators of cell polarity in yeast and animals (Etienne-Manneville and Hall, 2002). ARF family GTPases are required for several CDC42-mediated functions because human CDC42 is BFA sensitive and expression of a dominant-negative form of human ARF1 results in the redistribution of Golgi-localized human CDC42 to the cytosol (Erickson et al., 1996).

In comparison with yeasts and animals, Arabidopsis has many class 1 ARF proteins (Jürgens and Geldner, 2002; Vernoud et al., 2003). Transient expression of constitutively active (GTP-locked form) or constitutively inactive (GDP-locked form) mutants of ARF1 in tobacco (*Nicotiana tabacum*) and Arabidopsis cultured cells shows that this protein is required for the sequence-specific vacuolar sorting route to the lytic vacuole (Pimpl et al., 2003) and influences ER-to-Golgi transport as well as Golgi-derived transport to the plasma membrane, dependent on the cargo molecule (Lee et al., 2002; Takeuchi et al., 2002). Moreover, Arabidopsis ARF1 is able to complement and rescue the ARF1-ARF2 lethal yeast double mutant (Takeuchi et al., 2002). These results suggest that class 1 ARF proteins in Arabidopsis have similar cellular functions to their yeast and animal counterparts.

Here, we investigate developmental functions of Arabidopsis ARF1. As our expression and loss-of-function analysis suggests extensive redundancy, we expressed GTP- and GDP-locked mutants of ARF1 using region-specific and heat shock–inducible promoters and analyzed the consequences in the context of the multicellular organism. We demonstrate that class 1 ARF function is essential in plant development and that regulated expression of GTP- and GDP-locked mutants of ARF1 can be used to demonstrate roles of ARF1 in apical-basal polarity of epidermal cells and for ROP and PIN protein localization.

RESULTS

Arabidopsis Class 1 ARF Proteins Have Redundant Functions and Overlapping Expression Patterns

In Arabidopsis, six class 1 ARF proteins have been identified by the genome sequencing project. They share 98 to 100% amino acid identity with one another and conserved splice site positions (data not shown). Four of them can be grouped into two pairs derived from segmental genome duplication events (Jürgens and Geldner, 2002).

T-DNA insertion lines from the SIGNAL and the Syngenta GARLIC collections (McElver et al., 2001; Alonso et al., 2003; data not shown) revealed no obvious phenotypes, indicating extensive functional redundancy. Multiple RNA interference lines targeted to a common class 1 ARF sequence also revealed no specific phenotypes (data not shown).

If class 1 ARF proteins perform overlapping functions in Arabidopsis development, they should also share expression domains. We therefore created promoter fusions for all six class 1 ARF proteins using the ER-localized yellow fluorescent protein (ERYFP) as a reporter. For each promoter fusion, 20 independent transgenic lines were analyzed by confocal laser scanning microscopy (CLSM). ERYFP expression was observed in all the promoter fusion lines except for ARF6 (At5g14670), which is preferentially expressed in anthers and pollen (see Supplemental Figure 1A online). The promoter fusion lines for the other five class 1 ARF proteins showed essentially the same expression pattern with constitutive ERYFP expression in young seedlings (see Supplemental Figures 1B to 1F online), indicating extensive overlap of class 1 *ARF* gene expression.

We focused our studies on the Arabidopsis ARF1 (At2g47170) because this member has been studied at the cellular level (Lee et al., 2002; Takeuchi et al., 2002; Pimpl et al., 2003). GenBank EST expression data (http://www.ncbi.nih.gov/Genbank/) confirm that *ARF1* is expressed in all organs examined. To investigate tissue specificity of *ARF1* mRNA expression in different organs and at different developmental stages, we created *ARF1* promoter fusions using β-glucuronidase (GUS) as a reporter. GUS activity was detected throughout the roots of all the transgenic lines examined (see Supplemental Figure 1G online). In addition, we also observed strong GUS activity in vascular bundles, leaf primordia, stomata, trichomes, style, stigmatic tissue, and young pollen (see Supplemental Figures 1H to 1J online). Intense GUS activity was detected in embryo sacs and dissected embryos of all stages (see Supplemental Figure 1K online).

We investigated whether posttranscriptional regulation affected ARF1 expression by making stable transgenic Arabidopsis plants carrying the fusion construct of wild-type ARF1 (ARF1-WT) and enhanced green fluorescent protein (EGFP) under control of the Arabidopsis *ARF1* promoter (arf1-ARF1-WT-EGFP). Constitutive GFP expression was found in all the ARF1-WT-EGFP translational fusion lines. For example, GFP fluorescence was observed in all cells within the root meristem, and GFP fluorescence localized to the region of forming cell plate, to the growing root hairs, and also was detected in stomata and trichome cells (see Supplemental Figures 1L to 1P online). Collectively, our data suggest that the ARF1 protein is ubiquitously expressed and overlaps with the expression domain of the class 1 ARF members.

Arabidopsis ARF1 Localizes to Golgi Apparatus and Endocytic Organelles

In both yeast and mammalian cells, ARF1-Q71L (GTP-locked form) has significantly reduced GTPase activity and therefore behaves as a constitutively activated mutant (Pepperkok et al., 2000) that cannot hydrolyze its GTP and interferes with the sorting of membrane proteins into Golgi-derived COPI vesicles. ARF-T31N (GDP-locked form) has low affinity for GTP and has been shown to behave as a dominant-negative mutant (Dascher and Balch, 1994) that blocks the formation of COPI-coated vesicles. As the critical amino acids are conserved among class 1 ARF proteins (data not shown), both mutants are expected to also impair ARF1-mediated vesicle transport in plants. We made protein fusion constructs of ARF1-WT and the GTP- and GDP-locked dominant mutants of ARF1, namely ARF1-Q71L and ARF-T31N with EGFP, enhanced cyan fluorescent protein (ECFP), or enhanced yellow fluorescent protein (EYFP), under control of a *35S* promoter of *Cauliflower mosaic virus* (CaMV). We

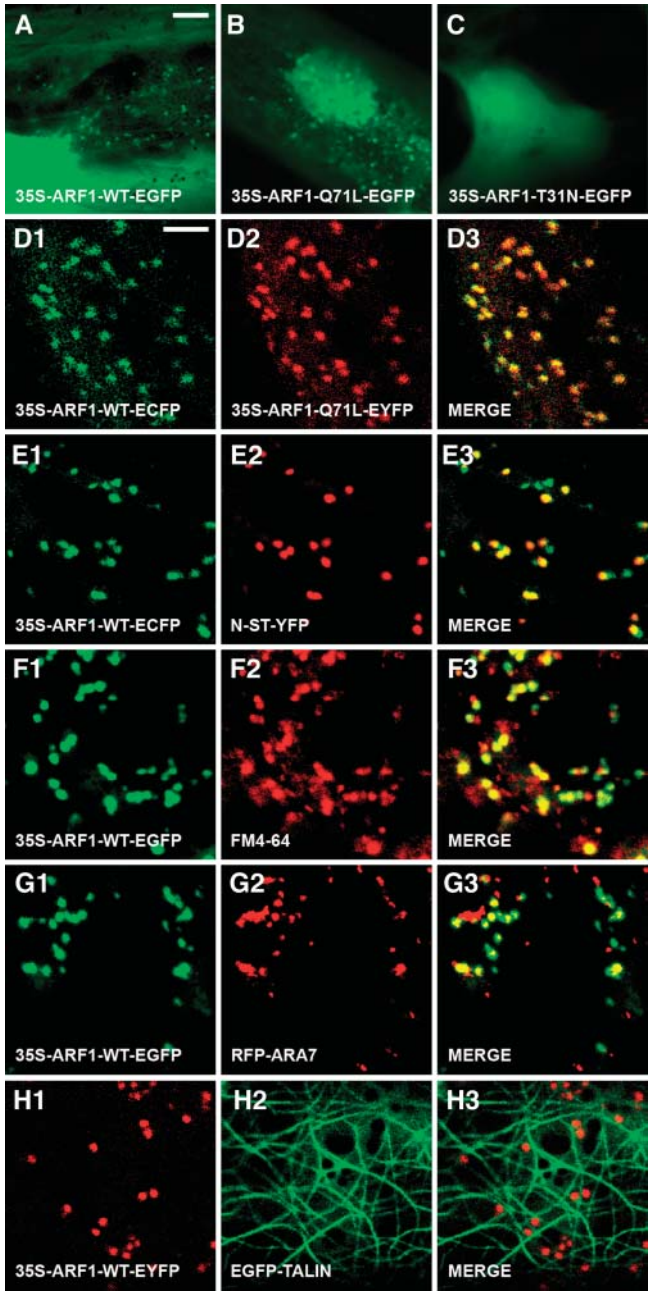

Figure 1. Transient Expression and Intracellular Localization of Arabidopsis ARF1 and Its Dominant Mutants in Onion Epidermal Cells.

(A) to **(C)** Transient expression of 35S-ARF1-WT-EGFP **(A)**, 35S-ARF1-Q71L-EGFP **(B)**, and 35S-ARF1-T31N-EGFP **(C)**.

(D1) to **(D3)** Colocalization analysis of 35S-ARF1-WT-ECFP (**[D1]**; green) and 35S-ARF1-Q71L-EYFP (**[D2]**; red). Merged image of **(D1)** and **(D2)** is depicted in **(D3)**. Note that all ECFP fluorescence coincides with EYFP fluorescence.

(E1) to **(E3)** Colocalization analysis of 35S-ARF1-WT-ECFP (**[E1]**; green) and N-ST-YFP (**[E2]**; red). Merged image of **(E1)** and **(E2)** is depicted in **(E3)**.

(F1) to **(F3)** Colocalization analysis of 35S-ARF1-WT-EGFP (**[F1]**; green) and FM4-64 (**[F2]**; red). Merged image of **(F1)** and **(F2)** is depicted in **(F3)**.

studied the intracellular localization and dynamics of the translocation of ARF1 protein during transient expression in onion (*Allium cepa*) epidermal cells. GTP-locked ARF1 colocalized with wild-type ARF1 in multiple punctuate structures, whereas no fluorescent motile organelles were observed in cells with GDP-locked ARF1 construct (Figures 1A to 1D; see Supplemental Movie 1 online).

Colocalization studies using ARF1-WT-EC/YFP and a resident Golgi protein *N*-α-2,6-sialyltransferase (N-ST) fused to YFP (N-ST-YFP; Grebe et al., 2003) or a Golgi-targeted *N*-acetylglucosaminyl (NAG) transferase fused to ECFP (NAG-ECFP) suggest that ARF1 largely resides in or associates with the Golgi apparatus but also localizes to organelles negative for the Golgi markers (Figure 1E; see Supplemental Figure 2A and Movies 2 to 4 online). The Golgi localization of ARF1 is in agreement with observations on maize (*Zea mays*) and tobacco cells using ARF1 antisera (Pimpl et al., 2000; Ritzenthaler et al., 2002). However, our data indicate that ARF1 localizes to additional sites. Indeed, we found that ARF1-WT-EGFP fluorescence partially overlaps with the endocytic marker FM4-64 (Figure 1F; see Supplemental Movie 5 online), which does not label Golgi apparatus in both onion and Arabidopsis cells (see Supplemental Figures 2B, 2D, and Movie 6 online), suggesting that Arabidopsis ARF1 is also localized to endocytic organelles. Furthermore, a subpopulation of ARF1 fluorescence coincides with a red fluorescent protein (RFP) fusion to the conventional type RAB5 homolog ARA7 from Arabidopsis (RFP-ARA7; Figure 1G; see Supplemental Movie 7 online) but not with a plant unique RAB GTPase ARA6 fused to EYFP (ARA6-EYFP; Ueda et al., 2001; see Supplemental Figure 2C and Movie 8 online), indicating that ARF1 and ARA7 reside in different endocytic organelles from ARA6. In addition, we found that ARF1-EYFP fluorescence moves along actin filaments, illustrated by an EGFP fusion to the mouse F-actin–binding protein TALIN (EGFP-TALIN; Kost et al., 1998; Figure 1H; see Supplemental Movie 9 online).

We next studied the intracellular localization of wild-type ARF1 and its mutated forms in transgenic Arabidopsis plants. A heat shock–inducible promoter from the Arabidopsis *HSP18.2* gene (Takahashi et al., 1993) was used to drive expression of the fusion proteins. Intense GFP expression was induced in Arabidopsis root cells within 2 h after heat shock induction (37°C, 2 h). Both heat shock–induced ARF1-WT-YFP and ARF1-Q71L-YFP distribute similar to arf1-ARF1-WT-EGFP (Figures 2A, 2B, and 2D1), suggesting that the heat shock promoter activity levels used did not alter protein localization. In hsp18.2-ARF1-T31N-ECFP lines, CFP fluorescence is largely cytosolic and localizes to the nucleus, whereas no moving organelles were labeled (Figure 2C). Colocalization analysis of ARF1-WT-GFP with Golgi and endocytic markers in Arabidopsis confirms our observations in

(G1) to **(G3)** Colocalization analysis of 35S-ARF1-WT-ECFP (**[G1]**; green) and RFP-ARA7 (**[G2]**; red). Merged image of **(G1)** and **(G2)** is depicted in **(G3)**.

(H1) to **(H3)** The fluorescence of 35S-ARF1-WT-EYFP (**[H1]**; red) is associated with the cortical network of actin filaments marked by EGFP-TALIN (**[H2]**; green). Merged image of **(H1)** and **(H2)** is depicted in **(H3)**. Bars = 25 μm in **(A)** for **(A)** to **(C)**, 5 μm in **(D)** for all other panels.

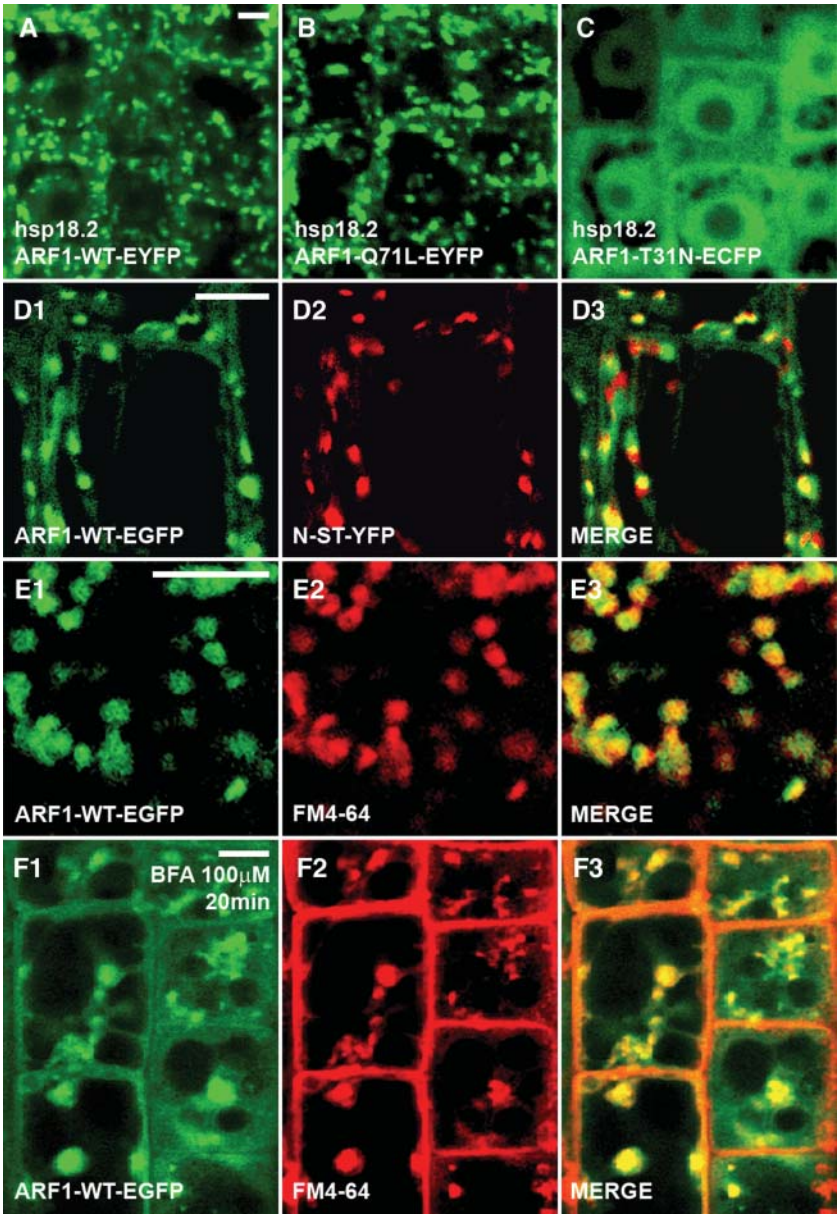

Figure 2. Expression and Intracellular Localization of Arabidopsis ARF1 and Its Dominant Mutants in Meristematic Root Epidermal Cells.

(A) to **(C)** Expression of hsp18.2-ARF1-EYFP **(A)**, hsp18.2-ARF1-Q71L-EYFP **(B)**, and hsp18.2-ARF1-T31N-ECFP **(C)** after heat shock (37°C, 2 h).
(D1) to **(D3)** Colocalization analysis of arf1-ARF1-WT-EGFP (**[D1]**; green) and N-ST-YFP (**[D2]**; red). Merged image of **(D1)** and **(D2)** is depicted in **(D3)**.
(E1) to **(E3)** Colocalization analysis of arf1-ARF1-WT-EGFP (**[E1]**; green) and the endocytosis marker FM4-64 (**[E2]**; red). Merged image of **(E1)** and **(E2)** is depicted in **(E3)**.
(F1) to **(F3)** Colocalization analysis of arf1-ARF1-WT-EGFP (**[F1]**; green) and FM4-64 (**[F2]**; red) at 20 min of incubation with 100 μM BFA. Merged image of **(F1)** and **(F2)** is depicted in **(F3)**.
Bars = 5 μm in **(A)** for **(A)** to **(C)**, in **(D1)** for **(D1)** to **(D3)**, in **(E1)** for **(E1)** to **(E3)**, and in **(F1)** for **(F1)** to **(F3)**.

onion epidermal cells (Figures 2D and 2E; see Supplemental Figures 2D and 2E online), and in addition ARF1-WT-GFP coaggregates with FM4-64 in BFA-induced compartments (Figure 2F). Taken together, our data suggest that ARF1 resides both in Golgi stacks and in a subpopulation of vesicles that move along actin filaments.

ARF1 Function in Arabidopsis Trichoblast Cells

The Arabidopsis root allows dissection of different aspects of cell polarity in plants. Distally, meristematic root cells divide in oriented planes. In the more proximal cell elongation and cell differentiation zones, trichoblast cells will develop root hairs at

their basal end, reflecting epidermal polarity along the apical-basal axis. Furthermore, root hairs elongate by polar tip growth. BFA treatment interferes with both aspects of epidermal polarity in a concentration-dependent manner (Grebe et al., 2002; Figures 4F and 4I), indicating that ARF-dependent processes are involved in apical-basal polarity and polar tip growth. In a search for specific ARF1 effects, we focused on polarity aspects of a single cell type: the trichoblast.

To dissect ARF1 functions, the GAL4-VP16 (GV)/UAS binary expression system (Brand and Perrimon, 1993) was used for region-specific expression of wild-type ARF1 and its mutated forms. Manipulation of ARF1 function in the root meristem using the root meristem–specific rch1GV driver affected root development, directional cell expansion, and cytokinesis (see Supplemental Figure 3 online), consistent with the expected household role of ARF1 in vesicle trafficking. However, it did not cause any obvious defects in root hair initiation and root hair tip growth (see Supplemental Figures 3C, 3F, 3H, and 3J online). We therefore specifically interfered with ARF1 function in trichoblasts. ARF1-WT and ARF1 mutants were expressed using a trichoblast-specific driver prp3GV whose expression is initiated at the onset of root hair outgrowth (Bernhardt and Tierney, 2000; Figure 3A). No alteration in apical-basal epidermal polarity or tip growth occurred in ARF1-WT–overexpressing lines (Figures 3B, 3G, 3L, and 3M), but trichoblast-specific expression of ARF1-Q71L or ARF1-T31N significantly inhibited tip growth (Figures 3C to 3F, 3H to 3K, 3N, and 3O).

Root hair formation can be completely abolished after strong heat shock induction (37°C, 4 h) in transgenic lines carrying hsp18.2GV and UAS-ARF1-Q71L or UAS-ARF1-T31N, whereas root hairs are normal in wild-type plants or ARF1-WT–overexpressing lines under the same conditions ($n = 100$; Figures 4A to 4C). Unlike in ARF1-T31N–expressing lines (Figures 4C and 4E), proper root hair formation recovers abruptly in ARF1-Q71L–expressing lines within 2 d, demonstrating that the effects of GTP-locked ARF1 on root hair formation are reversible (Figures

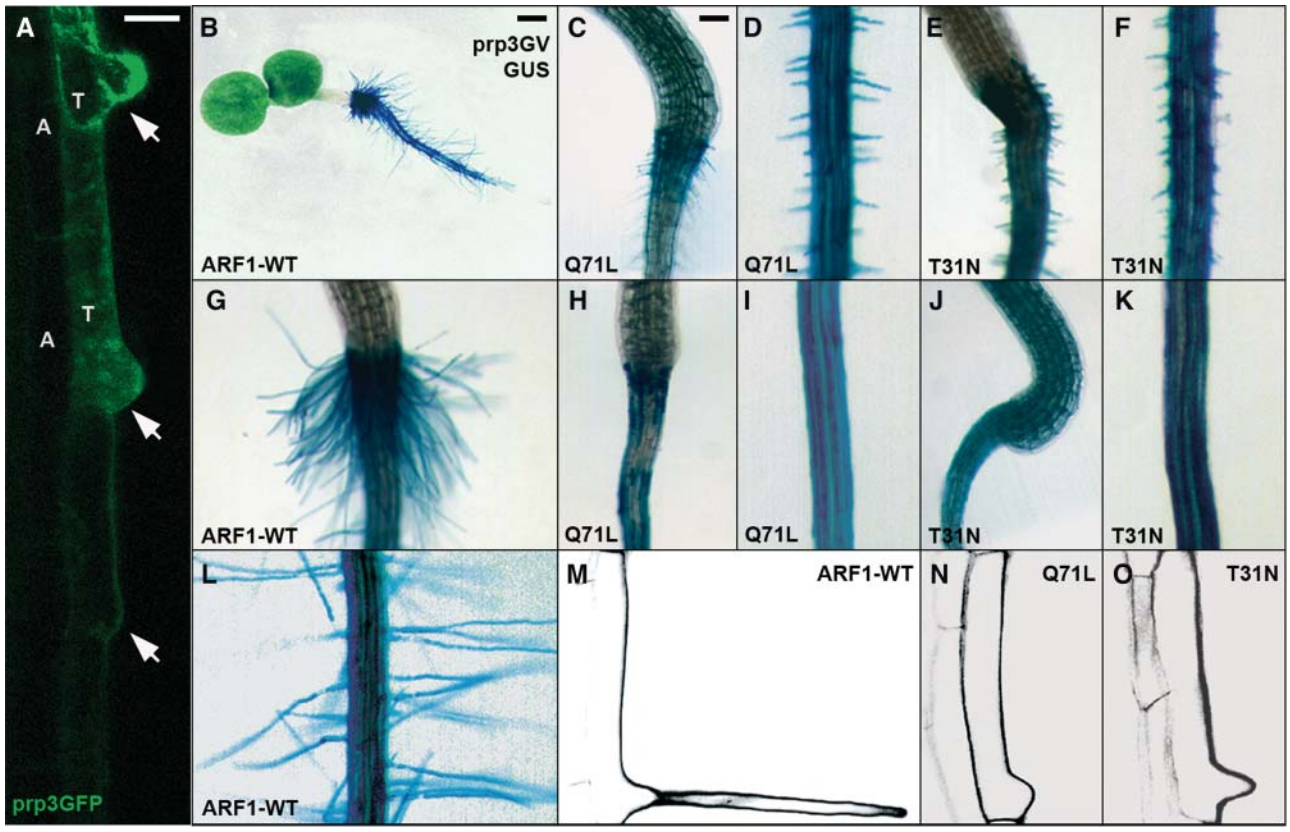

Figure 3. ARF1 Function Is Required for Root Hair Tip Growth in Arabidopsis Trichoblast Cells.

(A) Expression of the *GFP* reporter gene under the control of the trichoblast-specific *PRP3* promoter. Note that GFP expression is only observed in root hair–forming cells (T) but not in atrichoblast cells (A).

(B), **(G)**, and **(L)** Trichoblast-specific overexpression of ARF1-WT in transgenic lines carrying prp3GV and UAS-GUS, which is indicated by GUS staining.

(C) to **(K)** Trichoblast-specific expression of ARF1-Q71L (**[C]**, **[D]**, **[H]**, and **[I]**) and ARF1-T31N (**[E]**, **[F]**, **[J]**, and **[K]**). Note the graded root hair tip growth defects. Weak lines have very short root hairs (**[C]** to **[F]**), whereas strong lines have almost no root hair formation (**[H]** to **[K]**).

(M) to **(O)** Trichoblast cells in ARF1–overexpressing lines **(M)**, ARF1-Q71L–expressing lines **(N)**, and ARF1-T31N–expressing lines **(O)**. Images were obtained by CSLM.

Bars = 20 μm in **(A)** and **(M)** to **(O)**, 250 μm in **(B)**, and 100 μm in **(C)** and all other panels.

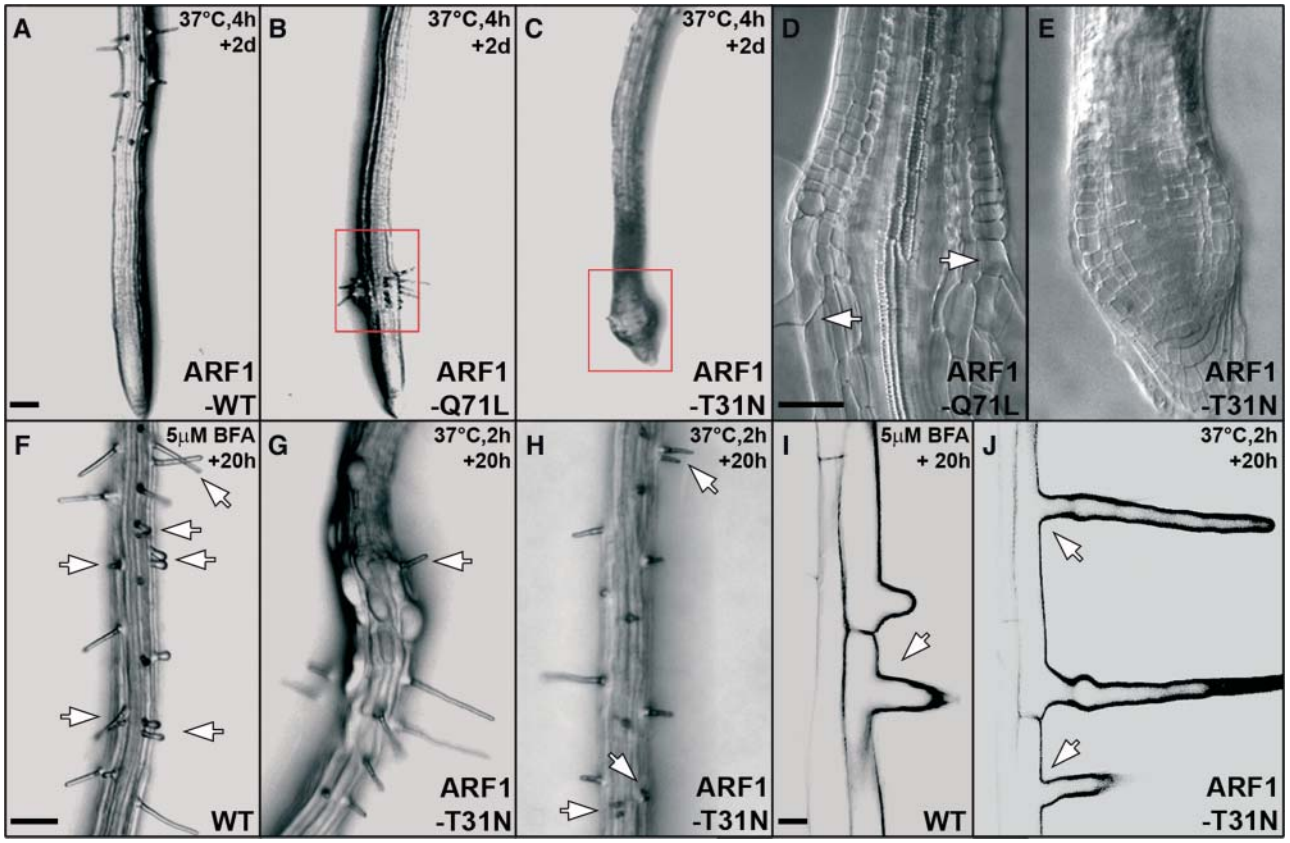

Figure 4. Heat Shock–Induced Expression of ARF1-Q71L and ARF1-T31N Strongly Affects Root Growth and Root Hair Formation.

(A) to **(E)** Root hair formation upon strong heat-shock induction (37°C, 4 h).
(A) to **(C)** Transgenic line carrying hspGV and UAS-ARF1-WT **(A)**, UAS-ARF1-Q71L **(B)**, or UAS-ARF1-T31N **(C)**. Root hair formation in ARF1-Q71L lines could recover within 2 d (**[B]**, boxed region). Abnormal root meristem in ARF1-T31N line is shown (**[C]**, boxed region).
(D) and **(E)** Enlarged views of boxed regions in **(B)** and **(C)**. Arrows in **(D)** indicate proper root hair formation.
(F) and **(I)** Root hair formation of Columbia wild-type line upon BFA treatment (5 μM, 20 h). Double root hairs (**[F]**, arrows) and apical-shifted root hair (**[I]**, arrow) were observed.
(G), **(H)**, and **(J)** Root hair formation in transgenic lines carrying hspGV and UAS-ARF1-T31N. Apical-shifted root hair (**[G]**, arrow), double root hairs (**[H]**, arrows), and a combination of both phenotypes (**[J]**, arrows) were observed. Bulging epidermal cells in **(G)** suggest deregulation of cell expansion.
Bars = 100 μm in **(A)** for **(A)** to **(C)**, 50 μm in **(D)** for **(D)** and **(E)**, 100 μm in **(F)** for **(F)** to **(H)**, and 20 μm in **(I)** for **(I)** and **(J)**.

4B and 4D). Root hairs are able to develop in ARF1-Q71L– and ARF1-T31N–expressing lines after mild heat shock induction (37°C, 2 h), but polarized root hair tip growth is significantly inhibited (Figures 4G, 4H, and 4J). These data suggest a dose-dependent effect of ARF1 manipulation on tip growth in Arabidopsis root hairs.

Consistent with the effect of BFA treatment (Grebe et al., 2002), apical-basal polarity in root hair initiation is dramatically affected by heat shock–induced expression of ARF1-T31N but not ARF1-Q71L (Figures 4G, 4H, and 4J). The difference in effect of the GTP- and GDP-locked mutants of ARF1 on epidermal polarity might indicate that they act on different targets, but can also reflect differences in protein level or stability. Apical-basal trichoblast polarity was not affected by the ARF1 mutants expressed in PRP3 or RCH1 expression domain as well as in the root cap region (data not shown). We concluded that root hair positioning in response to epidermal polarity and the decision to grow out a hair per se occur in the elongation zone.

ARF1 Function Is Required for ROP2 Localization and Action

The Arabidopsis *ROP2/ARAC4* gene has been implicated as a regulator of both apical-basal polarity in root hair initiation and polarized root hair tip growth. The *ROP2* gene is expressed throughout root hair development, and *ROP2* overexpression results in longer root hairs with multiple tips, whereas constitutively active GTP-bound ROP2 (ROP2-G14V) expression inhibits and depolarizes root hair tip growth (Jones et al., 2002). Transgenic lines carrying prp3GV and UAS-ROP2-G14V display the bulged root hair phenotype reported for 35S-ROP2 lines (Figures

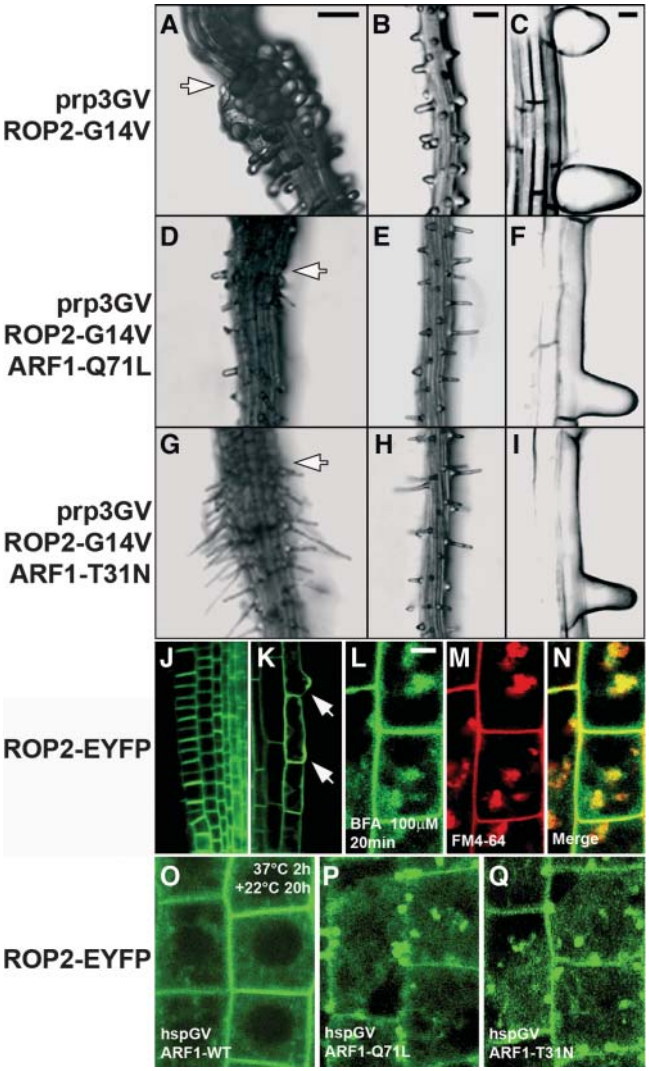

Figure 5. ARF1 Function Is Required for ROP2 Localization and Action.

(A) to **(I)** Root hair formation in transgenic lines carrying prp3GV and UAS-ROP2-G14V (**[A]** to **[C]**). Tip growth defect and strong isotropic expansion were observed in root hairs. Root hair formation in F1 lines carrying prp3GV, UAS-ROP2-G14V, and UAS-ARF1-Q71L is shown (**[D]** to **[F]**). Root hair formation in F1 lines carrying prp3GV, UAS-ROP2-G14V, and UAS-ARF1-T31N is shown (**[G]** to **[I]**). Note that root hair tip growth is strongly inhibited with no or much reduced isotropic expansion in F1 lines. Overview (**[A]**, **[D]**, and **[G]**), magnification (**[B]**, **[E]**, and **[H]**), and CSLM images (**[C]**, **[F]**, and **[I]**) are shown.

(J) and **(K)** Expression of the EYFP-ROP2 in Arabidopsis transgenic lines. YFP fluorescence is highly enriched in the apical and basal plasma membranes of the root meristematic cells, and localized to the future site of root hair formation as well as to the root hairs (**[K]**, arrows).

(L) to **(N)** Colocalization analysis of EYFP-ROP2 (**[L]**; green) and FM4-64 (**[M]**; red) in meristematic root epidermal cells of Arabidopsis transgenic lines at 2 h of incubation with 100 μM BFA. Merged image of **(L)** and **(M)** is depicted in **(N)**.

(O) EYFP-ROP2 localization in transgenic lines carrying hspGV and UAS-ARF1-WT after heat shock induction (37°C, 2 h, then 22°C, 20 h). Heat shock–induced ARF1 overexpression does not change EYFP-ROP2 localization.

5A to 5C), whereas no root hair phenotype was observed in transgenic lines carrying rch1GV and UAS-ROP2-G14V (data not shown).

BFA inhibits early polar localization of ROP proteins at the root hair initiation site, suggesting that root hair initiation requires an early-acting ARF-dependent process (Molendijk et al., 2001). To determine whether ARF1 function is involved in ROP2 action, we studied genetic interactions between *ARF1* and *ROP2* in trichoblast cells. We crossed UAS-ARF1-Q71L or UAS-ARF1-T31N into the transgenic lines carrying prp3GV and UAS-ROP2-G14V, and performed epistasis analysis in the F1 progeny. In all the F1 lines examined, root hairs showed tip growth defects but displayed no bulging (Figures 5D to 5I), indicating that ROP2 function in controlling polarized tip growth is ARF1 dependent.

We next investigated the localization of the ROP2 protein in Arabidopsis plants carrying the fusion construct of EYFP and ROP2 (EYFP-ROP2) under the control of the *ROP2* promoter. YFP fluorescence is highly enriched in the apical and basal plasma membranes of the root meristematic cells (Figure 5J), and consistent with its role in cell polarity, EYFP-ROP2 localized to the future site of root hair formation as well as to the tips of growing root hairs (Figure 5K). Moreover, EYFP-ROP2 partially colocalized with endocytic marker FM4-64 upon BFA treatment (Figures 5L to 5N), implying ARF-dependent ROP2 trafficking. Heat shock (37°C, 2 h)–induced overexpression of wild-type ARF1 had no obvious effects on the localization of the EYFP-ROP2 fusion protein (Figure 5O). However, in ARF1-Q71L– or ARF1-T31N–expressing lines, localization of the EYFP-ROP2 fusion protein was significantly altered within 20 h after heat shock induction, illustrated by strong internalization and reduced YFP fluorescence on the plasma membrane (Figures 5P and 5Q). These results suggest that ARF1 function is required for ROP2 localization.

ARF1-Q71L and ARF1-T31N Act Rapidly on Golgi Trafficking and FM4-64 Uptake but Slowly on PIN2 Localization

Delocalization of ROP2 after ARF1 manipulation was not clearly observed until 20 h after heat shock, which posed the question whether dominant ARF1 mutants act slowly on all ARF1-dependent processes or whether ROP2 localization defects might require intermediate steps. To assess whether heat shock–induced ARF1 mutants can rapidly affect known vesicular trafficking pathways in the intact plant, we analyzed changes in the distribution of Golgi markers, a functional auxin efflux component PIN2-EGFP fusion, and the endocytic marker FM4-64. As a control, we timed the delocalization response of these markers to ARF-GEF inhibition by BFA treatment.

(P) and **(Q)** EYFP-ROP2 localization in transgenic lines carrying hspGV and either UAS-ARF1-Q71L **(P)** or UAS-ARF1-T31N **(Q)** after heat shock induction (37°C, 2 h, then 22°C, 20 h). Note that internalized YFP fluorescence was observed within the cells.

Bars = 100 μm in **(A)** for **(A)**, **(D)**, and **(G)**; 100 μm in **(B)** for **(B)**, **(E)**, and **(H)**; 20 μm in **(C)** for **(C)**, **(F)**, and **(I)** to **(K)**; and 10 μm in **(L)** for **(L)** to **(Q)**.

No changes were observed in the distribution of any marker after the overexpression of ARF-WT at all heat shock periods used (Figures 6A, 6E, 6I, 6M, 6Q, and 6U). However, within 3 h of heat shock at 37°C, fluorescence of the two Golgi markers N-ST-YFP and NAG-EGFP was significantly altered in both ARF1-Q71L– and ARF1-T31N–expressing lines (Figures 6B, 6C, 6F, and 6G). Surprisingly, PIN2-EGFP was visibly internalized only after prolonged heat shock (Figures 6J, 6K, 6N, and 6O), suggesting that PIN2 exocytosis responds slowly to ARF1 manipulation.

We found almost no internalization of FM4-64 after 3 h of induction of ARF1-Q71L and ARF1-T31N expression (Figures 6R and 6S), and almost no vacuoles were labeled by FM4-64 within 3 h of heat shock at 37°C when FM4-64 was added before heat shock induction (Figures 6V and 6W). Thus, uptake of FM4-64 at the plasma membrane and endocytic trafficking of FM4-64 from endocytic organelles to the vacuole are affected, consistent with the inhibition of endocytosis by GTP-locked human ARF1 (Zhang et al., 1994).

BFA treatment affects the localization of Golgi markers within 15 min to 1 h (Figures 6D and 6H), consistent with the rapid changes observed upon ARF1 modulation. However, PIN2-EGFP, a slow responder to ARF1 modulation, responds rapidly to BFA (Figures 6L and 6P). More strikingly, the response to BFA of the endocytic marker FM4-64 differs from its response to ARF1 manipulation because BFA strongly interferes with endocytic trafficking of FM4-64 from endocytic organelles to the vacuole but not with FM4-64 uptake (Figure 6T and 6X). This might suggest that ARF1 modulates uptake through interaction with a BFA-insensitive ARF-GEF.

DISCUSSION

In Arabidopsis, multiple almost identical ARF1 family members exist, but their highly similar expression domain and the lack of mutant phenotypes in individual knockouts suggest that all family members have extensively shared functions. Expansion of gene families hampers straightforward dissection of context-specific roles during multicellular development. Moreover, complete knockouts of central players of the secretory system often lead to male gametophytic or embryonic lethality, which makes it very difficult to analyze their precise cell-biological roles (Zizioli et al., 1999; Sanderfoot et al., 2001). Yet, studies on ARF interactors and their inhibitors suggest that the ARF system serves such context-specific roles, as illustrated by recent investigations on the GNOM/EMB30 ARF-GEF and its link to polar auxin transport in planta (Geldner et al., 2003). Here, we use ARF1-WT and GTP- and GDP-locked dominant mutants of ARF1 (ARF1-Q71L and ARF1-T31N) to dissect roles of ARF1 in Arabidopsis. We show that manipulation of Arabidopsis ARF1 function in separate domains influences expected processes such as cytokinesis and tip growth. However, we also reveal specific modulation of apical-basal epidermal polarity in a distinct phase of development. At the molecular level, we show that the kinetics of inducible ARF responses can be used to separate direct and indirect effects on protein localization.

ARF1 has been shown to localize to Golgi apparatus in both mammalian and plant cells (Vasudevan et al., 1998; Pimpl et al., 2000; Ritzenthaler et al., 2002). Unexpectedly, we detected Arabidopsis ARF1 in endocytic organelles, suggesting that it plays a role in the trafficking of endocytic vesicles like non-plant ARF1 (Gaynor et al., 1998; Gu and Gruenberg, 2000). Consistent with this notion, uptake and trafficking of the endocytic marker FM4-64 is inhibited by both GTP- and GDP-locked forms of ARF1. Moreover, a subpopulation of Arabidopsis ARF1 coincides with the RAB5 homolog ARA7 but not with ARA6 (Ueda et al., 2001).

The effects of the ARF-GEF inhibitor BFA suggest that ARF-dependent vesicle trafficking plays an important role in the establishment of apical-basal epidermal polarity and in root hair tip growth (Grebe et al., 2002). Here, we show that dominant mutants of ARF1 interfere with both aspects of cell polarity, raising the question whether ARF1 is a target for both BFA-sensitive ARF-GEF–dependent polarity changes.

Which effectors are important for these polarization events? We show that polar ROP2 localization to the hair tip and phenotypic activity of ROP2 in this region require ARF1 function. These data functionally support the idea that root hair initiation involves ARF1-dependent polar localization of the ROP proteins (Molendijk et al., 2001). The slow relocalization of ROP2 after ARF1 manipulation suggests that intermediate steps are involved and that ARF1 may not be the principal ARF regulated by BFA-sensitive ARF-GEFs in ROP2 trafficking. However, we cannot exclude the formal possibility that these slow kinetics reflect interference of ARF1 manipulation with unrelated pathways.

The auxin transport machinery and actin cytoskeleton have been implicated in the establishment of apical-basal trichoblast polarity (Masucci and Schiefelbein, 1994; Sabatini et al., 1999; Grebe et al., 2002; Ringli et al., 2002). Furthermore, auxin influx and efflux carriers are BFA sensitive, and actin-mediated vesicle trafficking is required for the recycling of auxin efflux carriers (Morris and Robinson, 1998; Geldner et al., 2001, 2003; Grebe et al., 2002, 2003). We show that ARF1 manipulation can affect apical-basal polarity and interferes with PIN2-EGFP recycling, indicating that auxin transport carriers require proper ARF function. However, dominant ARF1 mutant–mediated PIN2-EGFP internalization is slow compared with changes in Golgi and endocytic markers, whereas PIN2-EGFP is among the fastest responders to BFA. These observations raise the possibility that ARF1 also influences vesicular cycling of auxin efflux carriers in an indirect way, whereas GNOM and/or other BFA-sensitive ARF-GEFs interact with another ARF member that is more directly involved in PIN recycling. Our findings suggest that ARF1 may not be the most BFA-sensitive target in polarization events involving ROP and PIN proteins, and they illustrate that caution needs to be exerted in inferring direct interactions from developmental phenotypes upon ARF manipulation.

Further dissection of specific ARF1-mediated processes will be required to reach a better understanding of its role in multiple distinct polarization events. A spectrum of interacting proteins, such as ARF-GEFs and ARF-GAPs, can provide specificity to ARF1 action. Furthermore, connected trafficking pathways may be secondarily affected, and these will have to be identified in each case. Our tissue-specific approach for ARF1 misregulation defines a ready-to-go system to search for specific vesicle transport components impinging on cell and tissue polarity by straightforward suppressor and enhancer screens.

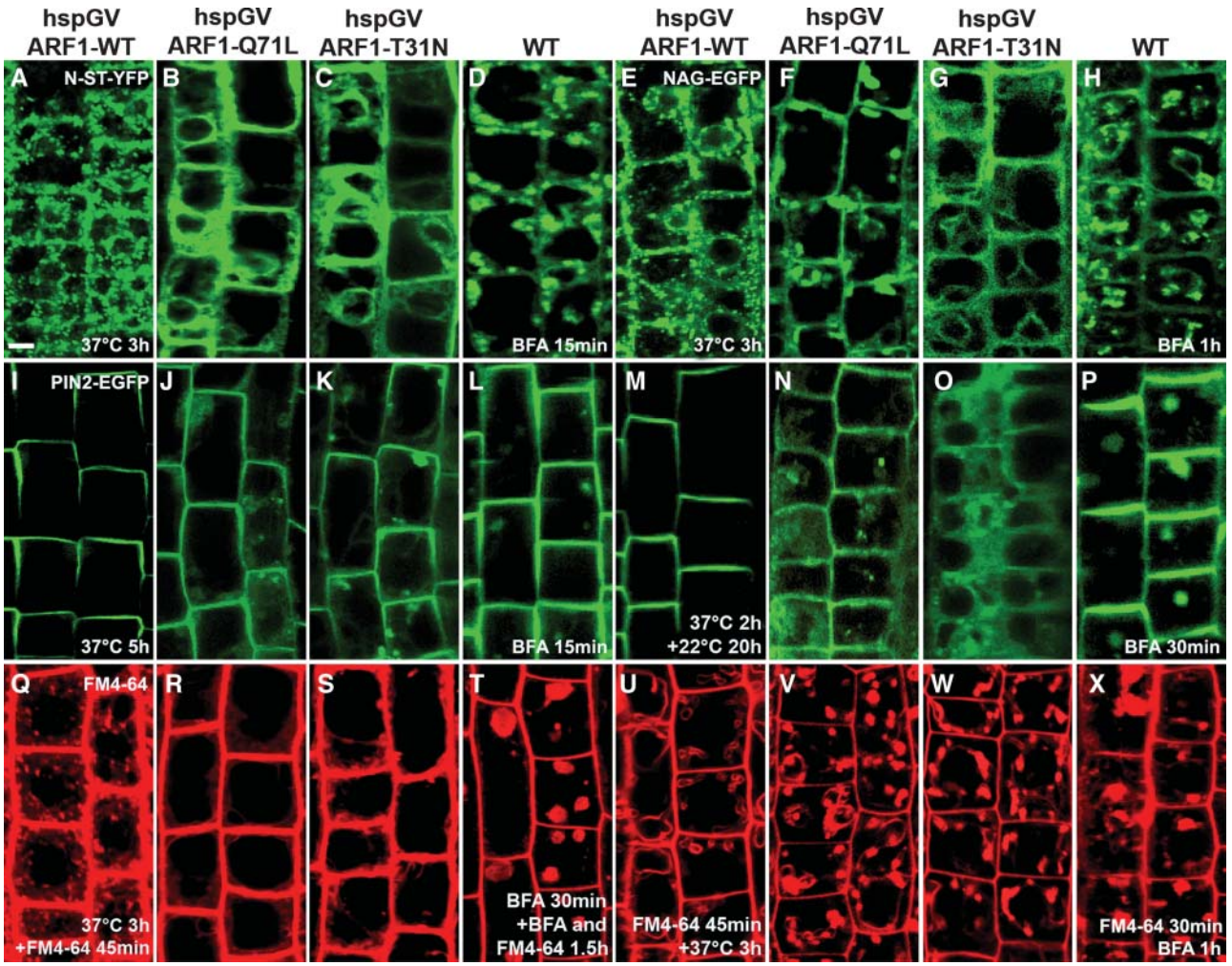

Figure 6. ARF1-Q71L and ARF1-T31N Act Rapidly on Golgi Trafficking and FM4-64 Uptake but Slowly on PIN2 Localization.

(A) to **(C)** N-ST-YFP localization in transgenic lines carrying hspGV and UAS-ARF1-WT **(A)**, ARF1-Q71L **(B)**, or ARF1-T31N **(C)** after heat shock induction (37°C, 3 h).
(D) N-ST-YFP localization after BFA treatment (50 μM, 15 min).
(E) to **(G)** NAG-EGFP localization in transgenic lines carrying hspGV and UAS-ARF1-WT **(E)**, ARF1-Q71L **(F)**, or ARF1-T31N **(G)** after heat shock induction (37°C, 3 h).
(H) NAG-EGFP localization after BFA treatment (50 μM, 1 h).
(I) to **(K)** PIN2-EGFP localization in transgenic lines carrying hspGV and UAS-ARF1-WT **(I)**, ARF1-Q71L **(J)**, or ARF1-T31N **(K)** after heat shock induction (37°C, 5 h).
(L) PIN2-EGFP localization after BFA treatment (50 μM, 15 min).
(M) to **(O)** PIN2-EGFP localization in transgenic lines carrying hspGV and UAS-ARF1-WT **(M)**, ARF1-Q71L **(N)**, or ARF1-T31N **(O)** after heat shock induction (37°C, 2 h, then 22°C, 20 h).
(P) PIN2-EGFP localization after BFA treatment (50 μM, 30 min).
(Q) to **(S)** FM4-64 staining in transgenic lines carrying hspGV and UAS-ARF1-WT **(Q)**, ARF1-Q71L **(R)**, or ARF1-T31N **(S)** after heat shock induction (37°C, 3 h) and then incubation with FM4-64 (5 μM, 45 min).
(T) FM4-64 staining after BFA treatment (100 μM, 30 min) and then incubated with 100 μM BFA and 5 μM FM4-64 for 1.5 h.
(U) to **(W)** FM4-64 staining in transgenic lines carrying hspGV and UAS-ARF1-WT **(U)**, ARF1-Q71L **(V)**, or ARF1-T31N **(W)** after incubation with FM4-64 (5 μM, 45 min) and then heat shock induction (37°C, 3 h).
(X) FM4-64 staining after incubation with FM4-64 (5 μM, 30 min) and then with 100 μM BFA for 1 h.
Bars = 10 μm.

METHODS

Plant Growth Conditions

Arabidopsis thaliana seeds were sterilized with the vapor-phase sterilization protocol described at http://plantpath.wisc.edu/~afb/vapster.html and imbibed for 4 d at 4°C in the dark, then germinated on vertically oriented plates containing half-strength MS agar (Duchefa, Haarlem, The Netherlands) and 1% sucrose, pH 5.8, and grown in a plant room at 22°C with a 16-h-light/8-h-dark cycle.

Plasmid Construction and Plant Transformation

ARF1 and *ROP2* cDNA were amplified from an Arabidopsis cDNA library using PCR, and cDNA sequences were verified. Q71L and T31N mutations in ARF1 and the G14V mutation in ROP2 were introduced using a PCR-based site-mutagenesis strategy (Stratagene, La Jolla, CA).

For the arf1-ERYFP and arf1-GUS promoter fusion constructs, 2.64 kb of upstream sequence from the Arabidopsis *ARF1* gene was fused to an *ERYFP* or *GUS* reporter gene and nopaline synthase terminator engineered in pGREENII-0229.

To make the arf1-ARF1-WT-EGFP, 35S-ARF1-WT-EGFP (or ECFP or EYFP), 35S-ARF1-Q71L-EGFP, 35S-ARF1-T31N-EGFP, hsp18.2-ARF1-WT-EGFP, hsp18.2-ARF1-Q71L-EYFP, and hsp18.2-ARF1-T31N-ECFP constructs, EGFP (or ECFP or EYFP) was fused in frame to the C terminus of ARF1 wild-type or mutant proteins. The resulting fusions were cloned into the pGREENII-0229 vector (http://www.pgreen.ac.uk) under the control of the Arabidopsis *ARF1* promoter, CaMV *35S* promoter, or Arabidopsis *HSP18.2* promoter (847 bp), respectively.

NAG-EYFP and NAG-ECFP were generated from NAG-EGFP (Grebe et al., 2003) by exchanging of EGFP to EYFP or ECFP. For ARA6-EYFP, *NAG* cDNA was exchanged for *ARA6* cDNA. To create EGFP-TALIN, the mouse TALIN F-actin–binding sequence from pSYC14 (a generous gift from N.H. Chua, Rockefeller University, New York, NY) was fused in frame to the C terminus of EGFP engineered in pGREENII-0229 between the CaMV *35S* promoter and nopaline synthase terminator.

To create the rch1GV construct, 2.7 kb of upstream sequence from the Arabidopsis *RCH1* gene (Casamitjana-Martinez et al., 2003) was fused to the GV coding sequence; the resulting construct also contained a UAS-ERGFP or UAS-GUS reporter engineered in the pGREENII-0029 vector. For prp3GV and hsp18.2GV constructs, 2 kb of Arabidopsis the *PRP3* gene promoter region or the Arabidopsis *HSP18.2* promoter sequence was subcloned before the GV coding sequence in the pGREENII-0029 vector with a UAS-GUS reporter. To generate UAS-ARF1-WT, UAS-ARF1-Q71L, UAS-ARF1-T31N, and UAS-ROP2-G14V plant transformation constructs, *ARF1* cDNA, ARF1-Q71L, ARF1-T31N, and ROP2-G14V were subcloned into a UAS cassette engineered in pGREENII-0229, and these constructs were transformed directly into the GV lines.

For the EYFP-ROP2 protein fusion, the EYFP coding sequence was fused in frame to N terminus of the Arabidopsis *ROP2* gene in pGREENII-0229 vector between 1.8 kb of the *ROP2* promoter sequence and 400 bp of the *ROP2* 3′-untranslated region. PIN2-EGFP was generated by insertion of EGFP into PIN2 (Luschnig et al., 1998; Muller et al., 1998) genomic fragment (nucleotides −2157 to 4380 from ATG) at position 2312. Its functionality was verified by the complementation of the *eir1-1* (*pin2*) agravitropic phenotype (Luschnig et al., 1998).

All the constructs were introduced into *Agrobacterium tumefaciens* strain C58C1 (GV3101) with the pSoup plasmid (http://www.pgreen.ac.uk) by electroporation. Plant transformation was done in Arabidopsis Columbia ecotype using the floral-dip method (Clough and Bent, 1998).

Histochemical Analysis of GUS Activity

Embryos and small seedlings were immersed in the staining solution (50 mM sodium phosphate buffer, pH 7.2, 0.1% Triton X-100, 1.5 mM potassium ferricyanide, 1.5 mM potassium ferrocyanide, and 1.5 mg/mL X-glucoronide) and incubated in the dark at 37°C. After staining, all the samples were cleared in 8:3:1 chloral hydrate:distilled water:glycerol and visualized using Nomarski optics on a Zeiss (Jena, Germany) Axioskop 2 microscope with a Nikon (Tokyo, Japan) DXM1200 digital camera.

Particle Bombardment–Mediated Transient Expression in Onion Epidermal Cells

For particle bombardment, all plasmids were amplified in *Escherichia coli* strain and purified using plasmid midi or mini kits according to the manufacturer's instructions (Qiagen, Valencia, CA). Onion (*Allium cepa*) bulb scale epidermis was bombarded with gold particles coated with plasmids using a Bio-Rad (Hercules, CA) PDS-1000/He particle delivery system. Bombarded specimens were incubated in water before CLSM analysis.

Inhibitor Treatments, FM4-64 Staining, and Analyses in Live Roots

BFA treatments were performed as described previously (Grebe et al., 2003). For FM4-64 stainings, onion epidermis or Arabidopsis seedlings were incubated in 2 mL of distilled water containing 5 μM FM4-64 for indicated periods at room temperature. Stained samples were washed twice with water and underwent heat shock treatment, or were directly observed by CLSM and/or two-photon LSM.

Microscopy

GFP, YFP, and CFP seedlings were visualized using a Leica (Wetzlar, Germany) MZ FLIII fluorescence stereomicroscope equipped with GFP and YFP filters. Propidium iodide (10 μg/mL in distilled water) was used to stain the cell walls of living root cells (red signal). Two-photon LSM and CLSM were used as described (Grebe et al., 2003).

ACKNOWLEDGMENTS

We thank Markus Grebe for inspiration and valuable discussions during this project. We also thank Nam-Hai Chua for generously providing the pSYC14 construct and Jenny Russinova for RFP-ARA7 construct; Renze Heidstra for providing the RCH1 promoter and GV system; and Anko de Graaff for help with two-photon LSM. We thank the Arabidopsis Biological Resource Center for providing seed stocks for SALK T-DNA insertion lines; the Salk Institute Genomic Analysis Laboratory for providing the sequence-indexed Arabidopsis T-DNA insertion lines; and Syngenta Biotechnology for providing Arabidopsis T-DNA SAIL seed lines (formerly known as GARLIC). This work is supported by a PIONIER Award of the Dutch Organization for Science.

Received October 9, 2004; accepted December 2, 2004.

REFERENCES

Alonso, J.M., et al. (2003). Genome-wide insertional mutagenesis of *Arabidopsis thaliana*. Science **301,** 653–657.

Balch, W.E., Kahn, R.A., and Schwaninger, R. (1992). ADP-ribosylation factor is required for vesicular trafficking between the endoplasmic reticulum and the cis-Golgi compartment. J. Biol. Chem. **267,** 13053–13061.

Bernhardt, C., and Tierney, M.L. (2000). Expression of AtPRP3, a proline-rich structural cell wall protein from Arabidopsis, is regulated by cell-type-specific developmental pathways involved in root hair formation. Plant Physiol. **122,** 705–714.

Brand, A.H., and Perrimon, N. (1993). Targeted gene expression as a means of altering cell fates and generating dominant phenotypes. Development **118,** 401–415.

Casamitjana-Martinez, E., Hofhuis, H.F., Xu, J., Liu, C.M., Heidstra, R., and Scheres, B. (2003). Root-specific CLE19 overexpression and the sol1/2 suppressors implicate a CLV-like pathway in the control of Arabidopsis root meristem maintenance. Curr. Biol. **13,** 1435–1441.

Chardin, P., and McCormick, F. (1999). Brefeldin A: The advantage of being uncompetitive. Cell **97,** 153–155.

Clough, S.J., and Bent, A.F. (1998). Floral dip: A simplified method for *Agrobacterium*-mediated transformation of *Arabidopsis thaliana*. Plant J. **16,** 735–743.

Dascher, C., and Balch, W.E. (1994). Dominant inhibitory mutants of ARF1 block endoplasmic reticulum to Golgi transport and trigger disassembly of the Golgi apparatus. J. Biol. Chem. **269,** 1437–1448.

Erickson, J.W., Zhang, C., Kahn, R.A., Evans, T., and Cerione, R.A. (1996). Mammalian Cdc42 is a brefeldin A-sensitive component of the Golgi apparatus. J. Biol. Chem. **271,** 26850–26854.

Etienne-Manneville, S., and Hall, A. (2002). Rho GTPases in cell biology. Nature **420,** 629–635.

Gaynor, E.C., Chen, C.Y., Emr, S.D., and Graham, T.R. (1998). ARF is required for maintenance of yeast Golgi and endosome structure and function. Mol. Biol. Cell **9,** 653–670.

Geldner, N., Anders, N., Wolters, H., Keicher, J., Kornberger, W., Muller, P., Delbarre, A., Ueda, T., Nakano, A., and Jurgens, G. (2003). The Arabidopsis GNOM ARF-GEF mediates endosomal recycling, auxin transport, and auxin-dependent plant growth. Cell **112,** 219–230.

Geldner, N., Friml, J., Stierhof, Y.D., Jurgens, G., and Palme, K. (2001). Auxin transport inhibitors block PIN1 cycling and vesicle trafficking. Nature **27,** 425–428.

Goldberg, J. (2000). Decoding of sorting signals by coatomer through a GTPase switch in the COPI coat complex. Cell **100,** 671–679.

Grebe, M., Friml, J., Swarup, R., Ljung, K., Sandberg, G., Terlou, M., Palme, K., Bennett, M.J., and Scheres, B. (2002). Cell polarity signaling in Arabidopsis involves a BFA-sensitive auxin influx pathway. Curr. Biol. **12,** 329–334.

Grebe, M., Xu, J., Mobius, W., Ueda, T., Nakano, A., Geuze, H.J., Rook, M.B., and Scheres, B. (2003). Arabidopsis sterol endocytosis involves actin-mediated trafficking via ARA6-positive early endosomes. Curr. Biol. **13,** 1378–1387.

Gu, F., and Gruenberg, J. (2000). ARF1 regulates pH-dependent COP functions in the early endocytic pathway. J. Biol. Chem. **275,** 8154–8160.

Jones, M.A., Shen, J.J., Fu, Y., Li, H., Yang, Z., and Grierson, C.S. (2002). The Arabidopsis Rop2 GTPase is a positive regulator of both root hair initiation and tip growth. Plant Cell **14,** 763–776.

Jürgens, G., and Geldner, N. (2002). Protein secretion in plants: From the trans-Golgi network to the outer space. Traffic **3,** 605–613.

Kost, B., Spielhofer, P., and Chua, N.H. (1998). A GFP-mouse talin fusion protein labels plant actin filaments in vivo and visualizes the actin cytoskeleton in growing pollen tubes. Plant J. **16,** 393–401.

Lee, M.H., Min, M.K., Lee, Y.J., Jin, J.B., Shin, D.H., Kim, D.H., Lee, K.H., and Hwang, I. (2002). ADP-ribosylation factor 1 of Arabidopsis plays a critical role in intracellular trafficking and maintenance of endoplasmic reticulum morphology in Arabidopsis. Plant Physiol. **129,** 1507–1520.

Lippincott-Schwartz, J., Yuan, L., Tipper, C., Amherdt, M., Orci, L., and Klausner, R.D. (1991). Brefeldin A's effects on endosomes, lysosomes, and the TGN suggest a general mechanism for regulating organelle structure and membrane traffic. Cell **67,** 601–616.

Lippincott-Schwartz, J., Yuan, L.C., Bonifacino, J.S., and Klausner, R.D. (1989). Rapid redistribution of Golgi proteins into the ER in cells treated with brefeldin A: Evidence for membrane cycling from Golgi to ER. Cell **56,** 801–813.

Luschnig, C., Gaxiola, R.A., Grisafi, P., and Fink, G.R. (1998). *EIR1*, a root-specific protein involved in auxin transport, is required for gravitropism in *Arabidopsis thaliana*. Genes Dev. **12,** 2175–2187.

Masucci, J.D., and Schiefelbein, J.W. (1994). The rhd6 mutation of *Arabidopsis thaliana* alters root-hair initiation through an auxin- and ethylene-associated process. Plant Physiol. **106,** 1335–1346.

Mayer, U., Buettner, G., and Juergens, G. (1993). Apical-basal pattern formation in the Arabidopsis embryo: Studies on the role of the gnom gene. Development **117,** 149–162.

McElver, J., et al. (2001). Insertional mutagenesis of genes required for seed development in *Arabidopsis thaliana*. Genetics **159,** 1751–1763.

Molendijk, A.J., Bischoff, F., Rajendrakumar, C.S., Friml, J., Braun, M., Gilroy, S., and Palme, K. (2001). *Arabidopsis thaliana* Rop GTPases are localized to tips of root hairs and control polar growth. EMBO J. **20,** 2779–2788.

Morris, D.A., and Robinson, J.S. (1998). Targeting of auxin carriers to the plasma membrane: Differential effects of brefeldin A on the traffic of auxin uptake and efflux carriers. Planta **205,** 606–612.

Mossessova, E., Corpina, R.A., and Goldberg, J. (2003). Crystal structure of ARF1*Sec7 complexed with Brefeldin A and its implications for the guanine nucleotide exchange mechanism. Mol. Cell **12,** 1403–1411.

Mostov, K., Su, T., and ter Beest, M. (2003). Polarized epithelial membrane traffic: Conservation and plasticity. Nat. Cell Biol. **5,** 287–293.

Muller, A., Guan, C., Galweiler, L., Tanzler, P., Huijser, P., Marchant, A., Parry, G., Bennett, M., Wisman, E., and Palme, K. (1998). *AtPIN2* defines a locus of *Arabidopsis* for root gravitropism control. EMBO J. **17,** 6903–6911.

Nebenfuhr, A., Ritzenthaler, C., and Robinson, D.G. (2002). Brefeldin A: Deciphering an enigmatic inhibitor of secretion. Plant Physiol. **130,** 1102–1108.

Pepperkok, R., Whitney, J.A., Gomez, M., and Kreis, T.E. (2000). COPI vesicles accumulating in the presence of a GTP restricted arf1 mutant are depleted of anterograde and retrograde cargo. J. Cell Sci. **113,** 135–144.

Pimpl, P., Hanton, S.L., Taylor, J.P., Pinto-DaSilva, L.L., and Denecke, J. (2003). The GTPase ARF1p controls the sequence-specific vacuolar sorting route to the lytic vacuole. Plant Cell **15,** 1242–1256.

Pimpl, P., Movafeghi, A., Coughlan, S., Denecke, J., Hillmer, S., and Robinson, D.G. (2000). In situ localization and in vitro induction of plant COPI-coated vesicles. Plant Cell **12,** 2219–2235.

Presley, J.F., Ward, T.H., Pfeifer, A.C., Siggia, E.D., Phair, R.D., and Lippincott-Schwartz, J. (2002). Dissection of COPI and Arf1 dynamics in vivo and role in Golgi membrane transport. Nature **417,** 187–193.

Ringli, C., Baumberger, N., Diet, A., Frey, B., and Keller, B. (2002). ACTIN2 is essential for bulge site selection and tip growth during root hair development of Arabidopsis. Plant Physiol. **129,** 1464–1472.

Ritzenthaler, C., Nebenfuhr, A., Movafeghi, A., Stussi-Garaud, C., Behnia, L., Pimpl, P., Staehelin, L.A., and Robinson, D.G. (2002). Reevaluation of the effects of brefeldin A on plant cells using tobacco Bright Yellow 2 cells expressing Golgi-targeted green fluorescent protein and COPI antisera. Plant Cell **14,** 237–261.

Sabatini, S., Beis, D., Wolkenfelt, H., Murfett, J., Guilfoyle, T., Malamy, J., Benfey, P., Leyser, O., Bechtold, N., Weisbeek, P., and Scheres, B. (1999). An auxin-dependent distal organizer of pattern and polarity in the Arabidopsis root. Cell **99,** 463–472.

Saint-Jore, C.M., Evins, J., Batoko, H., Brandizzi, F., Moore, I., and Hawes, C. (2002). Redistribution of membrane proteins between the

Golgi apparatus and endoplasmic reticulum in plants is reversible and not dependent on cytoskeletal networks. Plant J. **29,** 661–678.

Sanderfoot, A.A., Pilgrim, M., Adam, L., and Raikhel, N.V. (2001). Disruption of individual members of Arabidopsis syntaxin gene families indicates each has essential functions. Plant Cell **13,** 659–666.

Shaw, S.L., and Quatrano, R.S. (1996). The role of targeted secretion in the establishment of cell polarity and the orientation of the division plane in Fucus zygotes. Development **122,** 2623–2630.

Shevell, D.E., Leu, W.M., Gillmor, C.S., Xia, G., Feldmann, K.A., and Chua, N.H. (1994). EMB30 is essential for normal cell division, cell expansion, and cell adhesion in Arabidopsis and encodes a protein that has similarity to Sec7. Cell **77,** 1051–1062.

Spang, A. (2002). ARF1 regulatory factors and COPI vesicle formation. Curr. Opin. Cell Biol. **14,** 423–427.

Steinmann, T., Geldner, N., Grebe, M., Mangold, S., Jackson, C.L., Paris, S., Gälweiler, L., Palme, K., and Jürgens, G. (1999). Coordinated polar localization of auxin efflux carrier PIN1 by GNOM ARF GEF. Science **286,** 316–318.

Takahashi, T., Yabe, N., and Komeda, Y. (1993). Expression in yeast of a fusion gene composed of the promoter of a heat-shock gene from Arabidopsis and a bacterial gene for beta-glucuronidase. Plant Cell Physiol. **34,** 161–164.

Takeuchi, M., Ueda, T., Yahara, N., and Nakano, A. (2002). Arf1 GTPase plays roles in the protein traffic between the endoplasmic reticulum and the Golgi apparatus in tobacco and Arabidopsis cultured cells. Plant J. **31,** 499–515.

Ueda, T., Yamaguchi, M., Uchimiya, H., and Nakano, A. (2001). Ara6, a plant-unique novel type Rab GTPase, functions in the endocytic pathway of *Arabidopsis thaliana*. EMBO J. **20,** 4730–4741.

Vasudevan, C., Han, W., Tan, Y., Nie, Y., Li, D., Shome, K., Watkins, S.C., Levitan, E.S., and Romero, G. (1998). The distribution and translocation of the G protein ADP-ribosylation factor 1 in live cells is determined by its GTPase activity. J. Cell Sci. **111,** 1277–1285.

Vernoud, V., Horton, A.C., Yang, Z., and Nielsen, E. (2003). Analysis of the small GTPase gene superfamily of Arabidopsis. Plant Physiol. **131,** 1191–1208.

Zhang, C.J., Rosenwald, A.G., Willingham, M.C., Skuntz, S., Clark, J., and Kahn, R.A. (1994). Expression of a dominant allele of human ARF1 inhibits membrane traffic in vivo. J. Cell Biol. **124,** 289–300.

Zizioli, D., Meyer, C., Guhde, G., Saftig, P., von Figura, K., and Schu, P. (1999). Early embryonic death of mice deficient in gamma-adaptin. J. Biol. Chem. **274,** 5385–5390.